

Simulation of Secondary Metallurgical Processes Using Computational Thermodynamics and Comprehensive Statistical Learning Methods



Authors

Daniel Kavić (top left), Ph.D. Candidate, Steelmaking, K1-MET GmbH and Chair of Ferrous Metallurgy, Montanuniversität Leoben, Leoben, Austria
daniel.kavic@k1-met.com

Michael Bernhard (top right), Senior Scientist, Thermodynamics of Steelmaking, Chair of Ferrous Metallurgy, Montanuniversität Leoben, Leoben, Austria
michael.bernhard@unileoben.ac.at

Roman Rössler (bottom left), Senior Scientist, Steelmaking, R&D Metallurgy Department, voestalpine Stahl GmbH, Linz, Austria
roman.roessler@voestalpine.com

Christian Bernhard (bottom right), Associate Professor, Steelmaking and Casting, Chair of Ferrous Metallurgy, Montanuniversität Leoben, Leoben, Austria
christian.bernhard@unileoben.ac.at

Looking for more information on digitalization?

Visit AIST's free Digitalization Applications 101 module at AIST.org/DA101.

Digital technologies are transforming industry at all levels. Steel has the opportunity to lead all heavy industries as an early adopter of specific digital technologies to improve our sustainability and competitiveness. This column is part of AIST's strategy to become the epicenter for steel's digital transformation, by providing a variety of platforms to showcase and disseminate Industry 4.0 knowledge specific for steel manufacturing, from big-picture concepts to specific processes.

Introduction

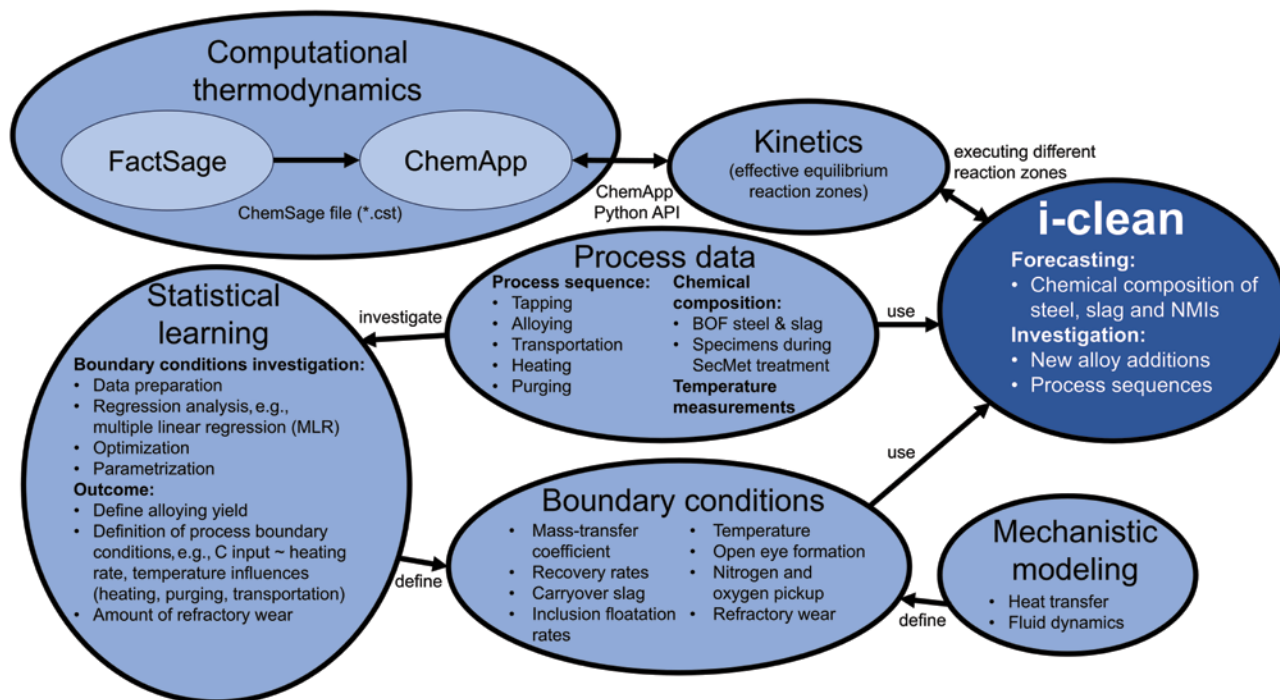
Given the urgent challenges facing the steel industry in the context of decarbonization, the significance of developing innovative solutions is becoming increasingly important. The transition to new production routes poses a significant challenge, particularly for the secondary metallurgical (SecMet) process, which acts as the final step before continuous casting. SecMet plays a decisive role for the final alloy composition and the modification of nonmetallic inclusions (NMI) in the steel and has, therefore, become indispensable in modern steel works. With the ongoing modernization of the steel industry and the increasing amount of data collected in recent years, opportunities are emerging to gain new insights through improved data mining and statistical learning methods as well as more efficient handling of large amounts of data. This new approach contributes to an improved understanding of the processes and optimization of the boundary conditions of classical thermodynamic models. Numerous works on solely data-driven modeling of SecMet processes (e.g., temperature models and alloy yield models) can already be found in the literature.¹⁻⁴ On the other hand, many complex kinetic and thermodynamic models describe the individual SecMet aggregates.⁵⁻⁸ This work intends to show how these

two disciplines can be combined to take the modeling of metallurgical processes to the next level. Fig. 1 illustrates the concept of the current project and how thermodynamic modeling will benefit from the statistical analysis of large amounts of production data. The presented work is divided into two packages: The first one deals with the development of a desktop application ("i-clean") to simulate the SecMet process from the tapping at the basic oxygen furnace (BOF) until the ladle furnace (LF). The second part is dedicated to a comprehensive statistical analysis to investigate the yield rates of different alloy additions at the LF and how the heating process could act as a carbon source.

The following chapters describe the software architecture and the implementation of the individual boundary conditions. In addition, a description will be given of how large amounts of data were processed and which methods were used to acquire new knowledge from the data-driven approach. Subsequently, the results from the statistical analysis are discussed. Finally, for the sake of demonstration, a use case for SecMet treatment is simulated, and the results of calculations are compared to the actual measured values.

Figure 1

The hybrid (data-driven, mechanistic and thermodynamic) model concept.



Description of “i-clean” Software

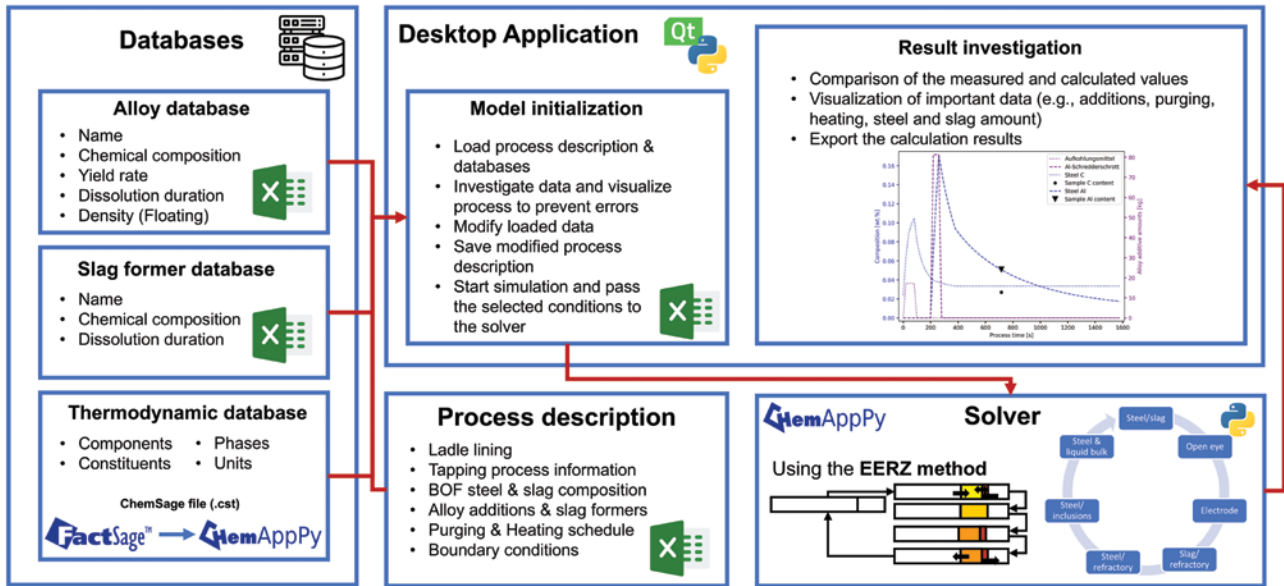
To simulate the SecMet process (from BOF tapping to LF), a desktop application called “i-clean” was developed in Python. This application uses an interface via ChemApp™ Python to the thermodynamic software database FactSage™ and is based on the concept of the effective equilibrium reaction zone (EERZ).⁷ The software architecture of the GUI application is shown in Fig. 2. The application itself can be divided into the following three sections.

The *preprocessing* module enables the automatic loading or manual entry of all input parameters and required data for the simulation. It is also possible to export and reload modified process sequences. Essential input data are the three databases “alloy database,” “slag former database” and “thermodynamic database.” The first one defines all compositions of the individual alloy additions that may be added throughout the simulated SecMet process. In addition, the dissolution duration and density of the material is given. Based on the density, it is possible to determine whether an alloy addition will be found in the liquid steel or whether it will float and will be located at the steel/slag interface. Furthermore, each alloy addition is given a unique name as an identification key. The “slag former database” contains the same information as already mentioned for the “alloy database.” The only difference is that the density is not needed, as it is assumed that slag formers will go directly to the slag.

The aforementioned two databases are defined as Excel files and imported automatically by the software. The “thermodynamic database” is made available as a ChemSage™ file (*.cst) by exporting it via FactSage and reading it via the ChemApp Python interface. The ChemSage file contains all information regarding the selected components, phases and units. Besides the databases, the software application also requires a detailed process description of the SecMet treatment. This includes the material additions (kg), the purging time ($\text{Nm}^3 \text{h}^{-1}$), and all the temperature trends based on the actual temperature measurements at the respective process step, as well as the heating power (kWh) at the LF. It is important to point out that all events contain the actual timestamp recorded at the steel plant. Moreover, each process phase (e.g., tapping, transport or ladle furnace) is defined according to the production logs, allowing the individual material additions and ladle treatments to be allocated to the respective ladle station in the simulation. The quantity of tapped steel at the BOF and the carryover slag must be defined. Further process information that is required for a calculation is the ladle radius and the composition of the refractory lining of the ladle in the steel and slag area. Finally, the metallurgical process boundary conditions (e.g., mass transfer coefficient, inclusion floatation rate, refractory wear, etc.) as well as the initial steel and slag composition must be specified. The composition corresponds to the measured analysis at the end of the BOF process just before tapping.

Figure 2

Representation of the software architecture of the Python GUI application “i-clean.”



As components, the major elements of the steel (e.g., C, Si, Mn, S, P, Cr, Al, Ti, O) and the main components of a SecMet slag (e.g., CaO, Al₂O₃, SiO₂, MgO, MnO, FeO) are considered.

The solver applies the EERZ method⁷ and, thus, couples thermodynamics with kinetics. The implementation of the EERZ method makes it possible to describe the change in the chemical composition of the steel, the non-metallic inclusions, and the slag during the entire SecMet process. The EERZ method⁷ attempts to simplify complex kinetic processes. In contrast to the coupled reaction models, the mass transfer coefficient k_i is assumed to be identical for all species of a specific bulk material. This leads to Eq. 1, where RA (kg) is the reacting amount, k (m s⁻¹) is the overall mass transfer coefficient, A (m²) is the reaction area and Δt (s) is the time step:

$$RA = (k\rho A) \Delta t \quad (\text{Eq. 1})$$

As an example, the EERZ concept for the reaction zone between steel and slag is described in Fig. 3, where RA_{St} and RA_{Sl} define the input masses before the calculation of the thermodynamic equilibrium, and EA'_{St} and EA'_{Sl} reflect the material that is returned to the corresponding bulk after calculating the equilibrium.

The EERZs considered within a steel ladle and the flow chart for the SecMet process model solver are shown in Figs. 4a and 4b. At the start of the simulation, the respective process influences (e.g., material addition, heating, purging and the current temperature) are defined as boundary conditions for each time step Δt . At this point, it should be mentioned that the temperature boundary condition is based on a linear interpolation between the actual measured temperatures. Also, no complex dissolution models were implemented for the alloy additions and slag formers due to the nature of macroscopic modeling. An assumption is made that all material mixes homogeneously within the steel or slag, respectively. The dissolution is completed between 30 seconds

Figure 3

Schematic demonstration of the effective equilibrium reaction zone (EERZ) concept for the steel/slag reaction zone.

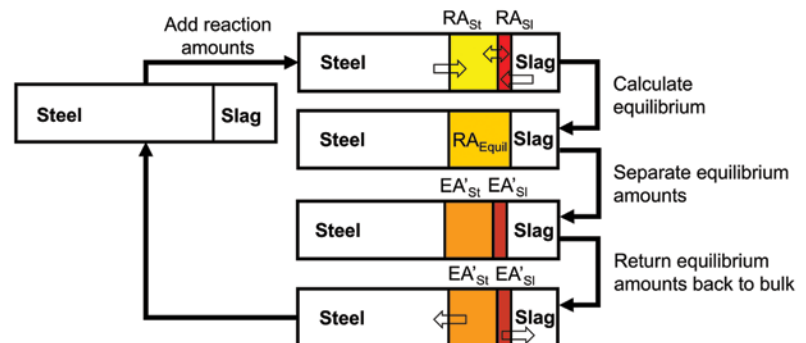
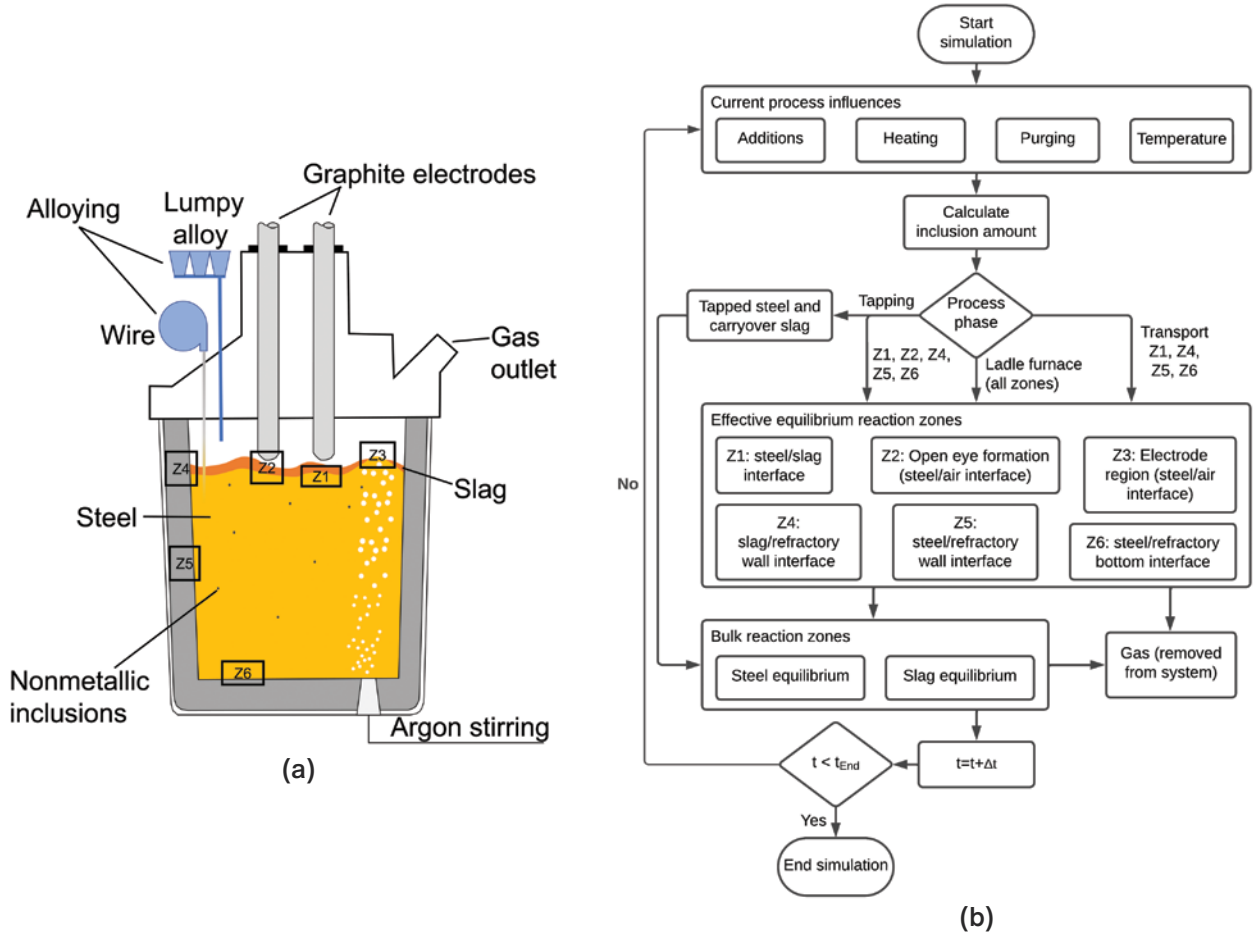


Figure 4

Considered EERZ within a steel ladle (a) and flow chart of the SecMet process model solver (b).



to 2 minutes, depending on the added material. Note that there are three different cases depending on which material is added. Alloy addition has a high density (floatation = false); the material is dissolved in the steel bulk. If the density is low and the addition floats, the alloy is added to zone 1 (steel/slag interface). In the present work, floating was only assumed for the two deoxidizers and alloying agents, Al and C. All slag formers are taken into account in the slag bulk equilibrium calculation. According to the flow chart, the next process step is the calculation of the current inclusion quantity. During the tapping phase, the inclusions are separated at a constant rate (after You et al.⁵), although it is evident that the actual rate depends on the inclusion size distribution and the flow conditions in the steel bath. This fitting parameter will be optimized in future studies using inclusion landscape data combined with the production data. For the ladle furnace, the deposition rate of the NMI is handled using Eqs. 2 and 3.⁹

$$\varepsilon = \left(\frac{nRT}{m} \right) \ln \left(\frac{P_t}{P_0} \right) \quad (\text{Eq. 2})$$

$$k_{float} = (0.57 \pm 0.15) \varepsilon^{(0.28 \pm 0.08)} \quad (\text{Eq. 3})$$

where

ε ($\text{W } \tau^{-1}$) = the effective stirring power per unit steel,
 n ($\text{mol } \text{s}^{-1}$) = the molar gas flowrate,
 R ($\text{J } \text{mol}^{-1} \text{K}^{-1}$) = the ideal gas constant,
 t (K) = the temperature,
 m (kg) = the weight of the steel,
 P_t (atm) = the total gas pressure at the bottom of the ladle,
 P_0 (atm) = the pressure at the melt surface and

k_{float} ($m s^{-1}$) = the purging rate-dependent deposition rate of the NMI.

The following simulation step examines the process phase (tapping, transport or ladle furnace). Different zones are executed depending on the selected process phase. Six zones between various interfaces are defined. Two additional reaction zones are required to calculate the thermodynamic equilibrium in the steel or slag bulk material. Zone 1 describes the reaction zone at the interface between the steel bath and the slag. For the tapping process, the mass transfer coefficient for the steel and the slag was defined according to You et al.⁵ For LF treatment, Eqs. 2 and 4 are used to describe the mass transfer coefficient k_{Steel} ($m s^{-1}$).⁹ The assumption is made that the mass transfer coefficient of the slag k_{Slag} ($m s^{-1}$) is one-twentieth of that of the steel due to its higher viscosity and lower diffusion properties (see Eq. 5).

$$k_{Steel} = (0.006 \pm 0.002) \epsilon^{1.4 \pm 0.09} \tag{Eq. 4}$$

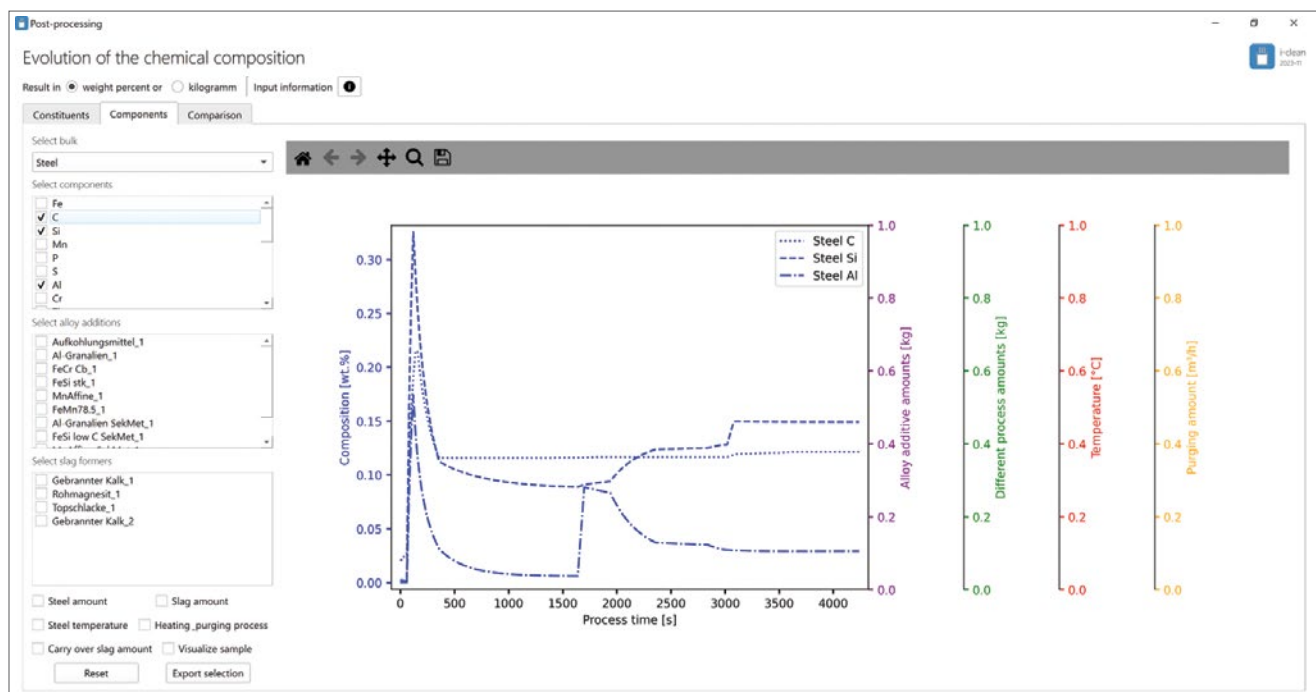
$$k_{Slag} = \frac{k_{Steel}}{20} \tag{Eq. 5}$$

For zone 2 (open-eye formation), the oxygen and nitrogen pickup into the steel is modeled according to Zhang et al.¹⁰ Here, the pickup depends on the purging rate. Within zone 3, carbon is added to the system due to thermal heating using carbon electrodes. For zones 4–6, measurements of refractory wear were carried out by the industrial partner voestalpine Stahl GmbH using the Ferrotron LaCam[®] system at different ladle lifetimes. An average wear rate of 50 kg of refractory material per melt was determined, with two-thirds of the material coming from the steel zone and a third from the slag refractory material. At the current stage of the software development, it is assumed that all of the refractory wear is due to erosion. Therefore, all of the material is deposited into the slag, although it is clear that there is some reaction between the refractory material and the steel/slag. This is currently being investigated and will be defined via different dissolution models and the EERZ approach. However, in the current software version, the 50 kg of worn material is distributed over the entire treatment period.

If the current simulation stage is the converter tapping process, zones Z1, Z2, Z4, Z5 and Z6 are applied. Furthermore, the amount of tapped steel and carryover slag per time step is transferred to the bulk material, which is subsequently considered when calculating the thermodynamic equilibrium for the bulk regions. With the ladle being transported from the tapping position to the ladle furnace, only zones Z1, Z4, Z5 and Z6 are

Figure 5

Postprocessing module of the i-clean software. Examination of individual components of the steel bulk.



applied. Once the ladle furnace treatment has started, all zones are performed simultaneously for each time step. After each reaction zone calculation, the gases produced (e.g., CO) are removed from the system, as they no longer participate in the process. Once the individual reaction zones have been carried out, the material of the EERZ is transported back to the respective bulk, whereby an additional equilibrium is calculated. Finally, the time step is increased by Δt , and the described procedure is repeated until the entire secondary metallurgical treatment has been simulated.

The *postprocessing* module enables a detailed graphical and numerical analysis of the results. Constituents or components of individual phases as well as the components of the respective bulk material can be plotted. Individual process influences such as alloy additions, steel melt temperature (based on actual temperature measurements), heating and purging quantities can also be represented. Furthermore, the steel and slag quantity development over the entire process can be displayed. The application offers the option of loading the measured steel and slag analyses and comparing the calculated compositions with them. Fig. 5 shows an example of the postprocessing module used to analyze the calculated C, Si and Al content over the entire SecMet process. Whenever there were abrupt changes in the alloying element profiles, the corresponding alloying agent was added to the melt.

Python version 3.9.7, PySide6 version 6.5.2, FactSage version 8.3, and ChemApp for Python version 8.2.3 were used to develop the software.

Statistical Analysis of Production Data

To determine the alloy yield rates of the individual additions and the influence of heating which acts as a carbon source, all influencing parameters must be predicted with a high level of accuracy using statistical methods. This critical step can be achieved by using a simple but powerful technique, multiple linear regression (MLR). Once the prediction model has been developed, one can use the estimated coefficients $\hat{\beta}_n$, and thus, calculate the variables of interest. The linear regression in the multidimensional case follows Eq. 6:¹¹

$$y = \hat{y} + e = \hat{\beta}_1 x_1 + \hat{\beta}_2 x_2 + \dots + \hat{\beta}_n x_n + e \quad (\text{Eq. 6})$$

where

\hat{y} = the estimated target vector,

x_n = the vector of an independent variable,

y = the actual measured value of the target variable and
 e = the residuals vector.

In general, an attempt is made to minimize the residuals vector e and thus obtain the best possible coefficients for the problem at hand. Note that an intercept variable was omitted for the entire modeling, as the prediction model was used to determine the change in the corresponding alloy element (Δy_{Alloy}). The formula for the calculation of Δy_{Alloy} (wt. %) corresponds to Eq. 7:

$$\Delta y_{\text{Alloy}} = \Delta y_{\text{Alloy,target}} - \Delta y_{\text{Alloy,initial}} \quad (\text{Eq. 7})$$

where

$\Delta y_{\text{Alloy,target}}$ (wt. %) = the last sample taken in the SecMet and

$\Delta y_{\text{Alloy,initial}}$ (wt. %) = the first sample taken in the SecMet.

A data-driven approach to define operational boundary conditions requires a large amount of data as there are many potential influencing factors during SecMet treatment. voestalpine Stahl GmbH provided the optical emission spectroscopy-pulse distributive analysis (OES-PDA) and process data for the entire annual production of 2022 to carry out the statistical investigation. This data set comprised 31,268 melts, whereby various data preparation and cleansing steps were carried out, which reduced the data set to 10,756 observations. The data set ultimately contained 116 steel grades, reflecting the majority of the fully Al-deoxidized steel grades. Only steel grades that were completely deoxidized with Al during the tapping process were examined in this study. The statistical data analysis also included the process influences of the Ruhrstahl-Heraeus vacuum plant, meaning that the yield rates determined should be valid for the entire SecMet process. Finally, the data preparation

Figure 6

Schematic illustration of a simplified secondary metallurgy (SecMet) treatment sequence.

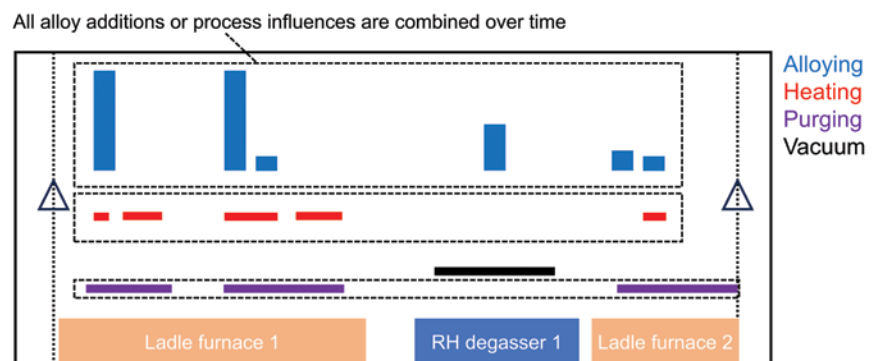
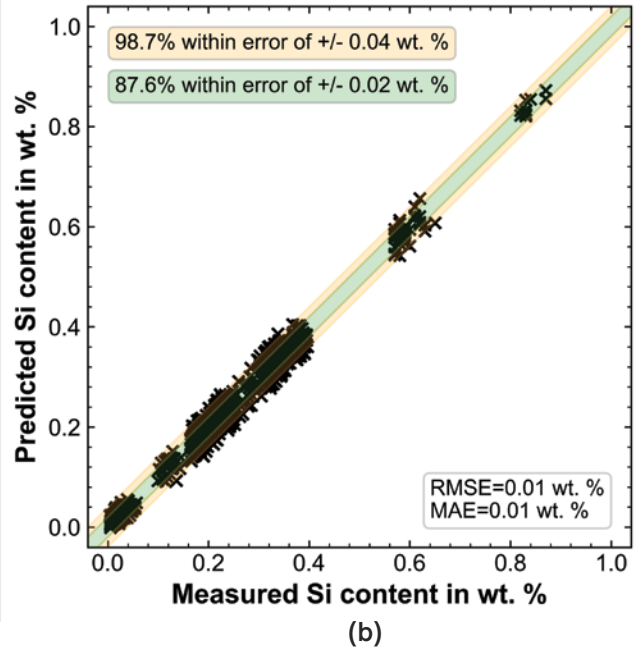
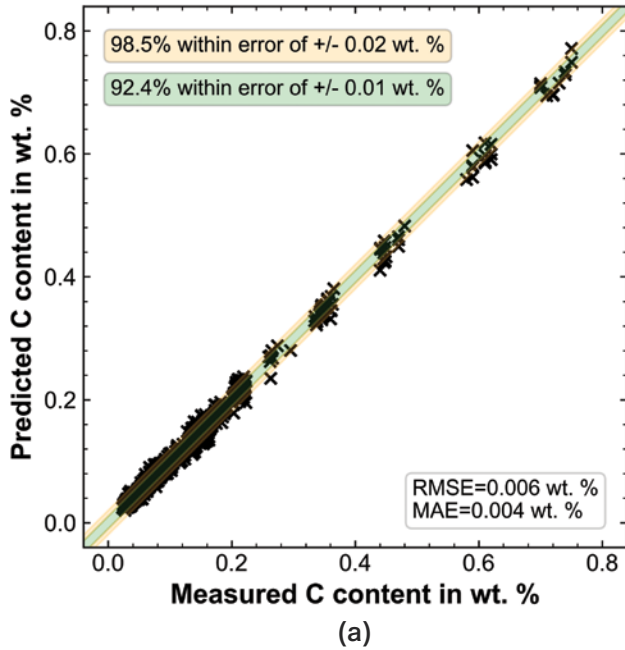


Figure 7

Comparison between the predicted and measured values for the carbon content (a) and the silicon content (b).



provided a data set that substantially simplifies the secondary metallurgical treatment. All material additions and process influences (e.g., heating, purging, vacuum treatment) between the first and last SecMet steel sample were accumulated and represented by one value per process influence (see Fig. 6). The statistical evaluation included the process influence parameters, the process duration, and approximately 25 other alloy additions could be considered as influencing parameters for further statistical analysis.

A train-validation-test data split of 60:30:10 was carried out to generalize better using the created prediction model. As mentioned earlier, the MLR was used for the statistical analysis. The iterative forward selection method was applied.^{12,13} The functionality of this selection method can be summarized as follows (where the parameter p represents the number of independent variables):

1. First, the null model M_0 is defined, which initially has no independent variables.
2. For $k = 1, 2, \dots, p - 1$:
 - a. Based on the M_k model, further $p - k$ models that use an additional variable are trained using the train data.
 - b. The model with the best goodness criteria based on the predictive ability using the validation data set is selected for each iteration step.

3. Select the best model of all iteration steps (M_0, \dots, M_k) with regard to the determined goodness criteria.

Since a model with a large number of variables always provides a better result for the R^2 , the quality criterion $R^2_{adjusted}$, which takes model complexity into account, was selected for this study. Based on the training data set, the degree of variance explanation, which directly impacts the number of selected influencing parameters, was chosen to be 0.95. Python version 3.9.7, numpy version 1.23.5, pandas version 1.5.2 and scikit-learn version 1.2.0 were used for statistical analysis.

Discussion of the Statistical Analysis Results

Due to the large number of alloying elements evaluated, only the C and Si prediction of the respective regression model is presented in detail in the following section. Nevertheless, Table 1 shows all yield rates determined during the investigation, which have been used for the simulation. It was found that the simplified approach describing the SecMet process route leads to outstanding results for all investigated alloying elements (except Al due to its usage as the main deoxidation element). The results of the MLR prediction for the two alloying elements using the test data set are illustrated in Figs. 7a and 7b. Note that the error bars in the two figures are only shown for better interpretability and in no way represent the tolerances specified by voestalpine Stahl GmbH.

Table 1

Yield Rates During the SecMet Treatment

Material name	Alloy yield rate [-]	Material name	Alloy yield rate [-]
Al-Granalia (during SecMet)	0.96	C (during SecMet)	0.98
SiMn	0.95	FeSi75	0.80
FeMn low. P	1	FeMn78.5	0.95
FeCr	1	MnAffine	0.934

The C-model proved excellent predictive ability with 92.4% and 98.5% of all predictions within the green and yellow error tolerances, respectively. For Si, 87.6% and 98.7% of the predictions could be found within the 0.02 and 0.04 wt. % deviation areas. The C or Si prediction model coefficients showed that all material additions where C, or respectively Si, has a major or minor share of the composition were identified as significant. Additionally, it could be determined for the carbon prediction that heating at the ladle furnace is associated with a low, however not neglectable, carbon input of 0.008 ppm per kWh.

The alloy yield rates can be calculated with the estimated coefficients, a mean ladle weight of 175 tons, and the average composition of the alloy addition. Those can be seen in Table 1. The evaluation showed that the mass balance is largely confirmed when alloying agents are added for a completely deoxidized steel in the ladle furnace. Only small amounts of the alloy additive end up in the slag due to oxidation. In the case of aluminum, the

model showed that the yield varies greatly depending on the addition time. At the beginning of the LF treatment, where higher amounts of less stable oxides in the slag and dissolved oxygen in the steel are still expected, an estimation of aluminum was difficult. However, aluminum yield rates close to 1 are achieved once the melt is completely killed. Only FeSi75 shows a lower value of 0.8 for the yield rate.

The C and Al addition yield rates during tapping differ significantly from those of the subsequent ladle treatment. This is partly due to the burn-off during the alloying process and the highly dissolved oxygen content in the steel. Another source of oxygen is the large quantity of carry-over slag from the converter, which has high proportions of FeO and MnO and, therefore, also contributes to the low yield. As no statistical analysis of the tapping process was carried out within the scope of the present work, literature values provided the required boundary conditions for this process stage.⁵

Discussion of Simulation Results

The calculation results of “i-clean” software will be discussed in this section for a selected case study carried out at voestalpine Stahl Linz. The simulation was done starting from tapping at the BOF to the end of the LF. The alloy yields were adjusted in the alloy database according to the new findings presented in the previous chapter. In addition, the influence of heating in terms of carbon input was also taken into account in the modeling. FactSage databases “FSstel”, “FToxid” and “FactPS” were used for the thermodynamic calculations. The initial and boundary conditions and all process influences for the simulation calculation can be found in Tables 2–9. Table 2 provides the steel composition at the end of the converter-blowing process. Table 3 describes the composition of the carryover slag. Fe_{Total} , Mn_{Total} and S_{Total}

Table 2

Steel Composition at the End of the Basic Oxygen Furnace Process

Element	wt. %	Element	wt. %
Carbon	0.0209	Aluminum	0.0000
Silicon	0.0020	Titanium	0.0010
Manganese	0.1250	Chromium	0.0160
Sulfur	0.0034	Oxygen	0.0607
Phosphorus	0.0080	Nitrogen	0.0027

Table 3

Carryover Slag Composition

Component	wt. %	Component	wt. %
CaO	46.88	P ₂ O ₅	1.24
SiO ₂	8.04	TiO ₂	0.35
MgO	7.59	Fe _{Total}	22.7
Al ₂ O ₃	0.01	Mn _{Total}	7.59
Cr ₂ O ₃	0.29	S _{Total}	0.03

Table 4

Process Boundary Conditions

Name	Value	Unit
Ladle radius	1.57	m
Tapped steel mass	172,000	kg
Carryover slag mass	600	kg
Time step	20	s

Table 5

Process Schedule During the SecMet Treatment

Process phase	Timestamp [min]	Duration [min]
Tapping	0	6
Transport	6	17
Ladle furnace	23	48

Table 6

Additions During SecMet Treatment

Name	Timestamp [min]	Amount [kg]	Name	Timestamp [min]	Amount [kg]
Carbon	1	24	MnAffine	3	2,593
Al-Granalía	2	314	FeMn78.5	3	1,406
Magensite	3	176	Al-Granalía	28	167
Lime	4	828	Lime	50	301
Top slag	4	297	FeSi	51	60
FeCr	3	327	MnAffine	51	267
FeSi	3	304	FeCr	51	203

Table 7

Purging Schedule

Timestamp [min]	Duration [min]	Rate [Nm ³ h ⁻¹]
3	3	70
33	7	90
48	15	90

Table 8

Heating Schedule

Timestamp [min]	Duration [min]	Amount [kWh]
24	1	390
28	3	1,013
51	5	1,502
56	2	510
59	3	1,003

Table 9

Measured Temperatures During SecMet Treatment

Time stamp [min]	Measured temperature [°C]
0	1,634
9	1,593
32	1,589
59	1,598
76	1,613

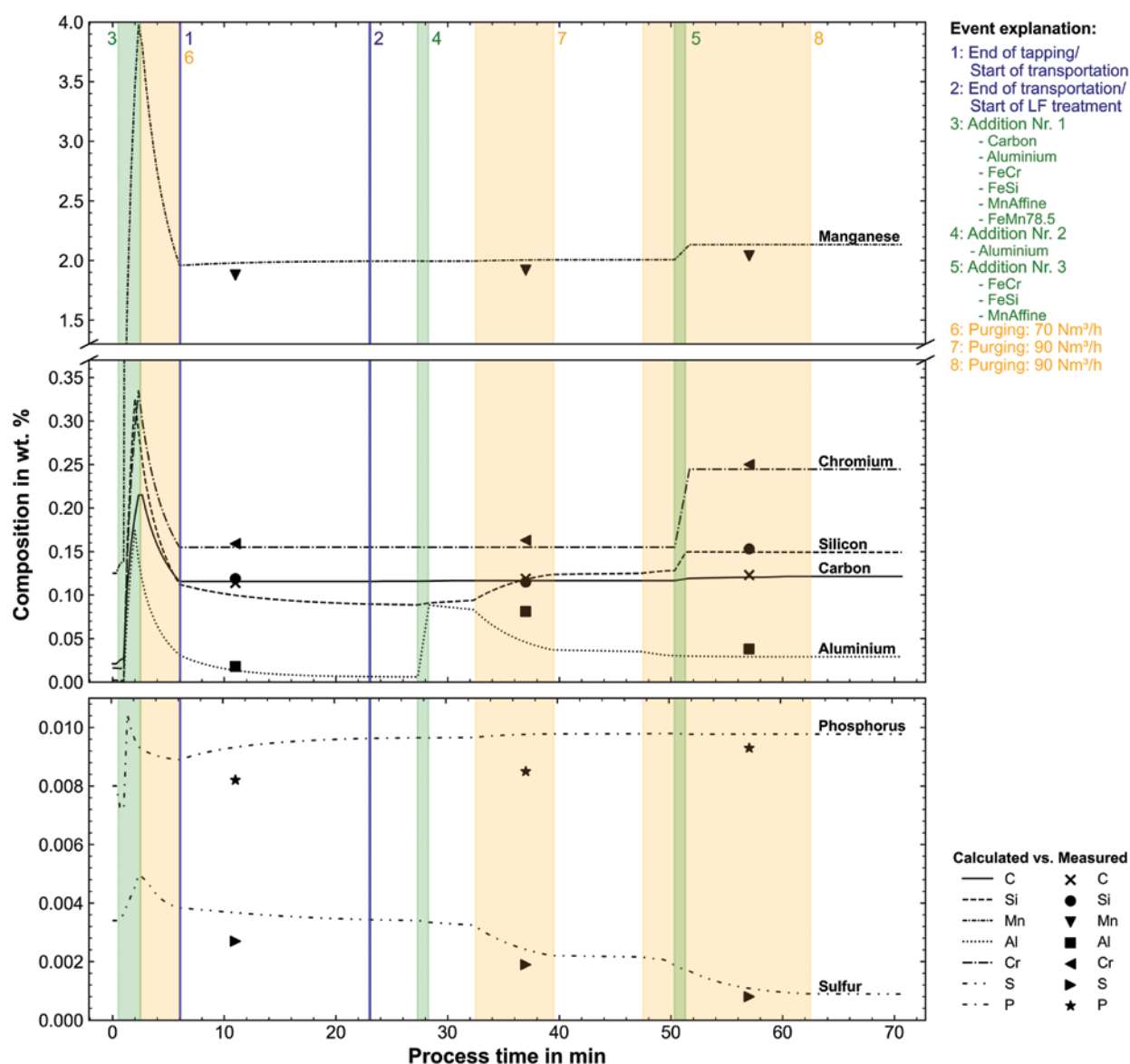
correspond to the total amount of the respective element in all compounds in the slag sample.

Table 4 describes the remaining boundary conditions the software requires, and Table 5 shows the schedule for the individual process phases.

Tables 6–8 contain all information regarding the process influencing parameters. In the SecMet treatment, preoxidation was carried out directly after tapping by adding C. Subsequently, Al was added as the main deoxidizing agent, followed by all other slag formers and alloying agents. Only small amounts of Al granules, FeSi, MnAffine, FeCr and lime were added during the ladle furnace treatment. Bottom purging was applied both during tapping and in the ladle furnace. A total of

Figure 8

Comparison of the simulated and the measured alloy contents over the entire SecMet process.



4,418 kWh over five arcing periods was required to heat the melt at the ladle furnace.

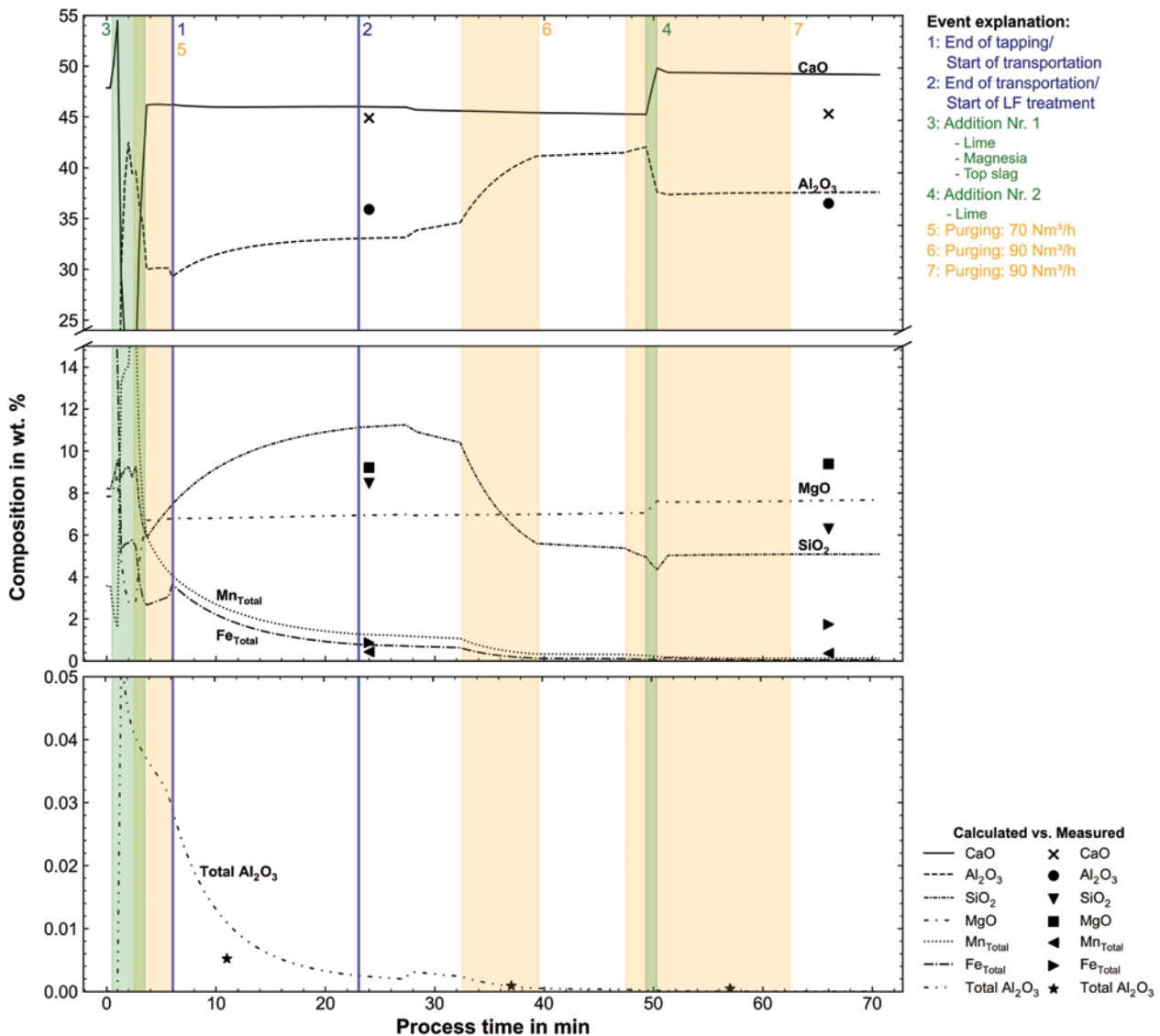
Finally, the simulation tool needs the actual temperature of the melt. The temperatures measured at the end of the converter process and during the SecMet treatment are shown in Table 9.

The results of the simulation calculation for the alloy and by-elements can be seen in Fig. 8. In addition, the process influences are also presented alongside them (except for heating, as this only significantly affects the carbon content in the current model). The results indicate good agreement between the calculated and measured values for all the main alloying elements. Due to the various additions directly at the beginning of the tapping

process, there is an immediate increase in the alloying element content. With the addition of Al, the entire melt is deoxidized and a large part of the unstable oxides (FeO and MnO) in the slag are reduced, so the mass balance broadly applies to all other elements. The additional tapped mass can explain the subsequent decrease of the individual alloy components during the further course of the process, which leads to a “dilution” of the melt. Upon entering the transport phase, the compositions largely stabilize. Nevertheless, it is worth noting once again that the nonmetallic inclusions formed are continuously removed from the melt, meaning that the total percentage of aluminum is constantly reduced. Furthermore, a slightly decreasing trend can be identified for Si and an

Figure 9

Comparison of the simulated and measured slag contents and the total Al₂O₃ in all nonmetallic inclusions over the entire SecMet process.



increasing trend for Mn. These trends can be explained by the interaction between the molten steel and the slag, as Si dissolved in the steel bath reacts with the MnO and the FeO from the slag. Once the ladle furnace is reached and Al is added, it significantly increases. Subsequently, the Al again reduces oxides from the slag. Here, the previously oxidized SiO₂ and the remaining MnO and FeO are removed from the slag. As expected, the simulation results reflect the ongoing kinetics and thus an interaction between steel and slag, especially during the purging gas treatment. At the end of the ladle treatment, the third alloying step occurs, whereby all target values are set as required.

Clear trends can be seen for the impurity elements P and S. The P₂O₅-rich carryover slag results in continuous rephosphorization throughout the process. On the other hand, the concentration of S continuously decreases as soon as the melt has been completely killed. The influence of the strong kinetics on desulfurization during the purging periods is obvious. If the measured and calculated alloy contents are compared, the results can be summarized as follows: The concentration of Mn is slightly overestimated by the simulation tool but still shows a maximum deviation of approximately 0.1 wt. % over the entire process; Cr could be determined with a maximum deviation of 100 ppm; for C, the deviation was even lower with a maximum of 25 ppm; the calculated Si content showed a deviation of 0.018 wt. % compared to the first sample taken. Later, the simulation result converged to within a few 10 ppm compared to the actual measured values; Al could also be predicted with high accuracy. In the second sample, Al showed a higher deviation (0.3 wt. %) from the measured value. At the two other measurement points, the deviation was significantly lower at less than 0.1 wt. %. The P content was 10 ppm higher at the first two sampling times. Toward the end of the SecMet treatment, the simulation result approaches the measured result to 5 ppm; for sulfur, the deviations are also 10 ppm at the beginning and decline over the entire SecMet process.

Fig. 9 shows the calculated and measured composition of the main slag components and the total Al₂O₃ over the treatment period. Various deoxidizing agents, alloying materials and slag formers are added at the beginning of the treatment, which initially results in very strong fluctuations in the slag composition. Once tapping is completed, the SiO₂ and Al₂O₃ content of the slag gradually increases, which is consistent with the results concerning the alloying elements in the steel bulk. The increase in SiO₂ and Al₂O₃ is counterbalanced by the reduction of MnO and FeO from the slag. If MnO and FeO are largely reduced from the slag, the SiO₂ is subsequently reduced back by Al₂O₃.

The increased kinetics due to the argon purging phases at the ladle furnace make this effect even more apparent. Finally, a small amount of lime is added at the ladle furnace, explaining the changes in the calculated

chemical compositions of the slag. From this final addition, a thermodynamic equilibrium between the steel and slag appears to have been largely established at the latest. As with the alloying elements, good agreement was generally achieved between the calculated results and the measured values. The CaO showed the highest deviations in the presented calculation. The difference between the measured and calculated values was about 1 wt. % for the first sample, but for the second sample it was already approximately 4 wt. %. Al₂O₃ was slightly underestimated by the calculation at the beginning (-3 wt. %); however, it becomes apparent that the values converged to 1 wt. % deviance toward the end of the simulation. For the MgO content, a discrepancy of 2 wt. % was achieved for both samples. For MnO and FeO, deviations of less than 2 wt. % were achieved, whereby the developed software assumes a complete reduction of the slag by the end of the calculation because of the continuous steel/slag interface reaction. One possible reason for the larger deviations might be that, in contrast to steel sampling, the slag sample is not taken automatically by a manipulator, but a small slag sample is taken manually from the surface of the slag. Obviously, this sampling procedure may lead to a greater deviation from the calculated results due to the inhomogeneous slag. As mentioned earlier, the nonmetallic inclusions in the steel were also taken into account in addition to the steel and slag compositions. However, it turned out that Al inclusions were almost exclusively present during the entire process due to the use of Al as the main deoxidizing agent. For this reason, the total Al₂O₃ content can be assumed to be representative for the total oxygen content in the steel. It also shows very good agreement with the measured OES-PDA data, and it becomes evident from both the simulation and the measured values that the number of nonmetallic inclusions continuously decreases throughout the process.

Summary and Conclusions

The present work deals with a hybrid approach using comprehensive simulation to predict the composition of steel, slag and nonmetallic inclusions in various secondary metallurgical process stages. For the simulation of SecMet processes, a new software named “i-clean” was developed in Python. It is based on the well-known coupled thermodynamic and kinetic EERZ models⁷ using the FactSage database via the ChemApp Python interface. In the first part, the developed software architecture, all implemented boundary conditions, and the features of the solver are discussed in detail. The work’s second part dealt with a data-driven approach to describe the alloy yields, and the influence of heating using carbon electrodes regarding the carbon input. The data evaluation was based on a comprehensive data set consisting of process and steel analysis data from an entire year’s production, which was provided for this work by voestalpine Stahl GmbH. Finally, the findings of the statistical

evaluation were used for the simulation of an exemplary case. This involved an attempt to simulate the development of the most important alloying and by-elements and nonmetallic inclusions, as well as the slag composition, for a melt produced at voestalpine Stahl GmbH. It was found that excellent results could be achieved for the steel composition compared to the samples taken. The simulation results of the slag composition showed a slightly higher deviation from the actual measured values, whereby the sampling of a possibly not completely homogenized slag must be considered as an error source. The development of the investigated aluminum inclusions showed a similar course to the actual measured values. The presented work demonstrates how novel data-driven approaches coupled with large amounts of data can be used to optimize existing thermodynamic and kinetic modeling further to simulate the SecMet process successfully. Other possibilities that will be investigated in future research based on the data-driven approach are the description of the process influences on the separation rate and formation of nonmetallic inclusions or the process dependency of the temperature, representing a critical boundary condition for thermodynamic calculation. Moreover, further

modeling measures must be implemented to optimize the EERZs between steel or slag and refractory.

Acknowledgments

The authors gratefully acknowledge the funding support of K1-MET GmbH, metallurgical competence center. The research program of the K1-MET competence center is supported by COMET (Competence Center for Excellent Technologies), the Austrian program for competence centers. COMET is funded by the Federal Ministry for Climate Action, Environment, Energy, Mobility, Innovation and Technology, the Federal Ministry for Labour and Economy, the Federal States of Upper Austria, Tyrol and Styria as well as the Styrian Business Promotion Agency (SFG) and the Standortagentur Tyrol. Furthermore, Upper Austrian Research GmbH continuously supports K1-MET. Beside the public funding from COMET, this research project is partially financed by the Montanuniversität Leoben and the industrial partners Primetals Technologies Austria, RHI Magnesita, voestalpine Stahl, and voestalpine Stahl Donawitz.

References

1. Z. Xin, J. Zhang, Y. Jin, J. Zheng and Q. Liu, "Predicting the Alloying Element Yield in a Ladle Furnace Using Principal Component Analysis and Deep Neural Network," *International Journal of Minerals, Metallurgy and Materials*, Vol. 30, No. 2, February 2023, pp. 335–344, <https://doi.org/10.1007/s12613-021-2409-9>.
2. X. Wang, "Ladle Furnace Temperature Prediction Model Based on Large-Scale Data With Random Forest," *IEEE/CAA Journal of Automatica Sinica*, Vol. 4, No. 4, April 2017, pp. 770–774, <https://doi.org/10.1109/JAS.2016.7510247>.
3. Z. Xin, J. Zhang, J. Zhang, J. Zheng, Y. Jin and Q. Liu, "Predicting Temperature of Molten Steel in LF-Refining Process Using IF-ZCA-DNN Model," *Metallurgical and Materials Transactions B*, Vol. 54, June 2024, pp. 1181–1194, <https://doi.org/10.1007/s11663-023-02753-0>.
4. Z. Xin, J. Zhang, J. Zheng, Y. Jin and Q. Liu, "A Hybrid Modeling Method Based on Expert Control and Deep Neural Network for Temperature Prediction of Molten Steel in LF," *ISIJ International*, Vol. 62, No. 3, March 2022, pp. 532–541, <https://doi.org/10.2355/isijinternational.ISIJINT-2021-251>.
5. D. You, C. Bernhard, P. Mayer, J. Fasching, G. Kloesch, R. Rössler and R. Ammer, "Modeling of the BOF Tapping Process: The Reactions in the Ladle," *Metallurgical and Materials Transactions B*, Vol. 52, June 2021, pp. 1854–1865, <https://doi.org/10.1007/s11663-021-02153-2>.
6. D. You, C. Bernhard, A. Viertauer and B. Linzer, "Simulation of the Refining Process of Ultra-Low Carbon (ULC) Steel," *Crystals*, Vol. 11, No. 8, July 2021, pp. 893, <https://doi.org/10.3390/cryst11080893>.
7. M-A. van Ende and I-H. Jung, "A Kinetic Ladle Furnace Process Simulation Model: Effective Equilibrium Reaction Zone Model Using FactSage Macro Processing," *Metallurgical and Materials Transactions B*, Vol. 48, February 2017, pp. 28–36, <https://doi.org/10.1007/s11663-016-0698-6>.
8. M-A. van Ende, Y-M. Kim, M-K. Cho, J. Choi and I-H. Jung, "A Kinetic Model for the Ruhrstahl Heraeus (RH) Degassing Process," *Metallurgical and Materials Transactions B*, Vol. 42, June 2011, pp. 477–489, <https://doi.org/10.1007/s11663-011-9495-4>.
9. K.J. Graham, "Integrated Ladle Metallurgy Control," Ph.D. thesis, McMaster University, 2008, p. 390.
10. Y. Zhang, Y. Ren and L. Zhang, "Kinetic Study on Compositional Variations of Inclusions, Steel and Slag During Refining Process," *Metallurgical Research & Technology*, Vol. 115, No. 4, October 2018, pp. 415–427, <https://doi.org/10.1051/metal/2018059>.
11. G. James, D. Witten, T. Hastie, R. Tibshirani and J.E. Taylor, *An Introduction to Statistical Learning: With Applications in Python*, Cham, Switzerland, Springer, 2023, pp. 69–83.
12. *ibid*, pp. 231–235.
13. G. Heinze, C. Wallisch and D. Dunkler, "Variable Selection — A Review and Recommendations for the Practicing Statistician," *Biometrical Journal*, Vol. 60, No. 3, May 2018, pp. 431–449, <https://doi.org/10.1002/bimj.201700067>. ◆